Heat and Mass Transfer in Fixed-bed Tubular Reactor

May 1st , 2008

Junichiro Kugai

Abstract

Heat and mass transfer problem in a fixed-bed tubular reactor is one of the major concerns in the chemical engineering. The two dimensional axial plug flow model was used for a water gas shift reactor to compare heat conduction or mass diffusion with convective effect. In the case of fast fluid flow in highly permeable catalyst-bed, convective heat transfer was dominant compared to heat conduction. Meanwhile both conductive mass transfer and mass diffusion were effective in mass transfer. Permeability had a large impact on homogeneity of fluid. A two dimensional particle-scale model was also investigated for detailed flow behavior. Mass distribution showed effective mixing of gas along radial direction due to high diffisivity of the gas, even when a low permeable and low porous catalyst particle was assumed.

1. Introduction

The design of catalyst particles for fixed-bed reactor is optimized by computational fluid dynamics (CFD). The CFD is used to obtain detailed flow and temperature fields in the reactor. In the field of reactor engineering, physical demands such as low pressure drop or high heat transfer efficiency are often in conflict with chemical demands such as gas contact efficiency [1]. Low tube-to-particle diameter ratio is needed for heat management, i.e. sufficient heat supply from the reactor wall for highly endothermic reaction or sufficient heat removal to the reactor wall for highly exothermic reaction [2]. Steam reforming of hydrocarbons is one of the examples, which is an endothermic reaction [3], while another is CO combustion, which is an exothermic reaction.

The early stage of reactor modeling has been based on simplifying assumption such as homogeneity, effective transport parameters, and pellet effectiveness factors [4, 5]. Homogeneity stands for viewing the fixed-bed as a single phase continuum. The assumption of effective or apparent transport parameters is based on the idea of unidirectional axial plug flow of the fluid throughout the reactor. These effective transport parameters are determined empirically, i.e. the parameters lump together all of the contributing physical phenomena. This assumption is still employed frequently in reactor modeling [6-9]. However, this approach has always caused inconsistency in the heat transfer coefficient or wall Nusselt number among a number of reported results. The inconsistency is originated from the lack of the local-scale flow picture of the bed. Recent magnetic resonance imaging (MRI) [10-13] have demonstrated that heat is transferred not solely by axial flow but also by strong radial convective flows as fluid is displaced around the packing elements.

Computational techniques for fluid flow have recently employed for reactor modeling as a alternative method to the above mentioned semi-empirical method, in attempting to understand detailed flow in the pore scale. The approach was validated by comparing apparent transport parameters with those from model-matching theory based on experimental measurements [8, 14, 15]. One of the outcome of CFD is a complex picture of strong radial flow. Local heat transfer rates was shown not to be correlated statistically with the local flow field [16]. The pressure and the wall temperature were found to have little or no influence on the apparent heat transfer parameters [17]. Addition of heat sinks to represent the thermal effects of chemical reaction have shown much larger effect on heat transfer performance than amount of internal voids in the particles [1].

One of the concerns in CFD is that all elements have a finite dimension in all edges, which does not allow actual contact points between solid parts in the geometry [4]. This limitation causes inconsistency of heat transfer coefficient with the one calculated by model-matching theory [17]. To avoid this, the diameter of the particles was slightly reduced in the model and finer mesh density was applied to wall-particle and particle-particle contact regions [2, 18]. The simulation implemented using a wall segment model with finer mesh in the contact regions gave good agreement with full bed simulation. Another concern is how to include chemical reactions in simulation. Inclusion of chemical reaction is so far limited to lattice Boltzmann simulation of isothermal flow with surface reaction [19, 20]. Heat sink was used to mimic the thermal effect of chemical reaction as mentioned above and the burden of calculation was reduced by using wall segment model for finite elemental approach. The challenge has always been how to correlate macro-scale behavior and particle-scale behavior.

In this study, a axial two dimensional tubular reactor model was built up using COMSOL and water gas shift reactor in a lab-scale was reproduced. The effects of average linear velocity of fluid, heat of reaction, permeability, porosity on distribution of velocity, temperature, and mass inside the tubular reactor were investigated. Also, particle-scale model was employed for investigating the balance between advection inside the particles and diffusion outside the particles.

2. Governing equations

An axial 2D model of a plug flow fixed-bed tubular reactor where the catalyst bed behaves as a porous media was assumed. Three components, velocity, temperature, and mass (CO concentration in the fluid) inside the tubular reactor were considered. The equations for each components were based on the report by Delhaye and Achard [21]:

$$\frac{\partial}{\partial t}(\rho_g v_r)+\frac{1}{r}\frac{\partial}{\partial r}(r\rho_g v_r v_r)+\frac{\partial}{\partial z}(\rho_g v_z v_r)=-\frac{\partial p}{\partial r}-f\frac{\rho|v|v_r}{d_p}+\frac{2}{r}\frac{\partial}{\partial r}\left(r\mu\frac{\partial v_r}{\partial r}\right)+\frac{\partial}{\partial z}\left(\mu\frac{\partial v_r}{\partial z}\right)-2\mu\frac{v_r}{r^2}+\frac{\partial}{\partial z}\left(\mu\frac{\partial v_z}{\partial r}\right) \quad \text{(Equation 1)}$$

$$\frac{\partial}{\partial t}(\rho_g v_z)+\frac{1}{r}\frac{\partial}{\partial r}(r\rho_g v_r v_z)+\frac{\partial}{\partial z}(\rho_g v_z v_z)=-\frac{\partial p}{\partial z}-f\frac{\rho|v|v_z}{d_p}+\rho_g g_z+\frac{1}{r}\frac{\partial}{\partial r}\left(r\mu\frac{\partial v_z}{\partial r}\right)+2\frac{\partial}{\partial z}\left(\mu\frac{\partial v_z}{\partial z}\right)+\frac{1}{r}\frac{\partial}{\partial r}\left(r\mu\frac{\partial v_r}{\partial z}\right) \quad \text{(Equation 2)}$$

$$\rho_g C_p \frac{\partial T}{\partial t} + \rho_g C_p v_z \frac{\partial T}{\partial z} + \rho_g C_p v_r \frac{\partial T}{\partial r} = \frac{\partial}{\partial z}\left(\lambda_{ea} \frac{\partial T}{\partial z}\right) + \frac{1}{r}\frac{\partial}{\partial r}\left(\lambda_{er} r \frac{\partial T}{\partial r}\right) + \sum_j (-\Delta H_{r,j}) r_j \rho_{cat} (1-\varepsilon)$$

(Equation 3)

$$\frac{\partial \rho_i}{\partial t} + \frac{\partial (\rho_i v_z)}{\partial z} + \frac{1}{r}\frac{\partial (r \rho_i v_r)}{\partial r} = \frac{\partial}{\partial z}\left(\rho_g D_{ea} \frac{\partial \omega_i}{\partial z}\right) + \frac{1}{r}\frac{\partial}{\partial r}\left(r \rho_g D_{er} \frac{\partial \omega_i}{\partial r}\right) - r_i \rho_{cat} (1-\varepsilon)$$

(Equation 4)

$$\frac{\partial \rho_g}{\partial t} + \frac{\partial (\rho_g v_z)}{\partial z} + \frac{1}{r}\frac{\partial (r \rho_g v_r)}{\partial r} = 0$$

(Equation 5)

The effect of water gas shift reaction was included in heat and mass transfer. However, the total molar amount of the gas was assumed constant, i.e. the fluid was assumed to be ideal gas, so that the equation of momentum balance is independent of those of heat and mass transfer. This assumption also simplifies the calculation of mass, i.e. only CO concentration is needed for consideration. The rate expression of water gas shift was based on Arrhenius equation as shown in Equation 6. The reaction orders for reactants and products were obtained from literature. The term of approach to equilibrium, β, was introduced so that it counts suppression of the reaction rate in the CO concentration range close to equilibrium. Although reaction orders, activation energy, pre-exponential factor are affected by temperature or mass concentration, they were assumed constant for simplification. Nonetheless, this rate expression realizes mutual interaction between heat and mass balance.

Water gas shift reaction: $CO + H_2O = CO_2 + H_2$

$$R\,(\text{rate}) = d\,c_{CO} / dt = -A \exp(-E_a/RT)\, a_{CO}^{0.1}\, a_{H2O}^{0.8}\, a_{CO2}^{-0.2}\, a_{H2}^{-0.6} (1-\beta) \quad \text{(Equation 6)}$$

$$\beta = (a_{CO2}\, a_{H2}) / (a_{CO}\, a_{H2O}\, K) \quad \text{(Equation 7)}$$

A : Pre-exponential factor for the reaction rate

E_a : Activation energy

R : Gas constant

c_{CO} : Concentration of CO

a_i : Fraction of gas component *I*

β : Approach to equilibrium

3. Formulation

A model of the fixed-bed tubular reactor was built in axial 2D code of COMSOL (Figure 1). The parameters of fluid and porous media were summarized in Table 2. These are all from databases and literature. The heat capacity (expressed as $kJ/m^3/K$) is similar for four gas components, suggesting convective heat flux is not so much affected by change of gas composition during reaction. Thermal conductivity is more influenced since H_2 has 5 to 10 times of thermal conductivity than the other gases, but the difference becomes smaller in high temperature. Therefore, these parameters were assumed independent of gas composition throughout the reactor. Thermal conductivity, heat capacity and mass diffusivity were modified using Equation 8 - 10 so that the properties represent the properties of gas-solid mixture. In the Equation 10, τ is tortuosity, which represents how much the distance between two points in the porous media compared to the length of straight line between these two points. According to literature, porosity and tortuosity are related. Table 1 represents calculated diffusivity in porous media as a function of porosity. Permeability was roughly estimated regarding the catalyst-bed as well-sorted sand.

$$k_{porous} = k_{gas}\,\varepsilon + k_{solid}\,(1-\varepsilon) \qquad \text{(Equation 8)}$$

$$Cp_{porpus} = Cp_{gas}\,\varepsilon + Cp_{solid}\,(1-\varepsilon) \qquad \text{(Equation 9)}$$

$$D_{porous} = (\varepsilon / \tau)\, D_{gas} \qquad \text{(Equation 10)}$$

Table 1 Gas diffusivity in porous media

ε	0.6	0.5	0.4	0.3	0.2
D_{porous}	2.7 x10^{-5}	2.0 x 10^{-5}	1.5 x 10^{-5}	0.9 x 10^{-5}	0.5 x 10^{-5}

Table 2 Values of parameters used in the simulation

Parameter [unit]	Value
ρ density [kg/m^3]	0.258
η viscosity [Pa s]	1 x 10^{-5}
ε porosity	0.4
κ permeability [m^2]	1 x 10^{-7}
k conductivity [W/m/K]	g : 0.1, s : 1.2, g-s : 0.76
C_p heat capacity [kJ/**m^3**/K]	g : 2.1, s : 525, g-s : 315
D diffusivity [m^2/s]	g: 6 x E^{-5}, g-s : 1.5 x10^{-5}
A pre-exponential factor	1 x 10^8
E_a activation energy [kJ/mol]	70
$\triangle H$ heat of reaction [kJ/mol]	-40

*g-s represents calculated value from Equation 8-10

The boundary condition also simulated the actual reaction condition. Figure 1 shows the boundary conditions for velocity, temperature, and CO concentration. The inlet gas composition was set to 13%CO-8%CO_2- 28%H_2O- 51%H_2, which corresponds to 2.542 mol/m^3 of CO concentration. The fluid velocity at inlet was assumed laminar flow with average velocity of 0.085 m/s.

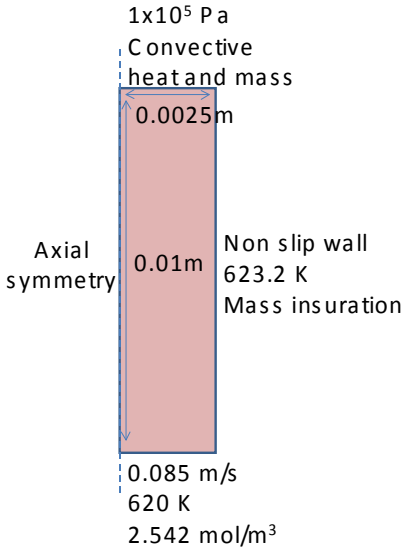

Figure 1 Tubular reactor model and boundary condition

4. Solution

Figure 2 is distribution of velocity, temperature, and CO concentration in the cross-section through the axis. The region of fluid velocity lower than average velocity is limited to within 350 μ m from the wall. This was narrower than the case of laminar flow without porous media in which the region extends to 750 μ m from the wall. The pressure drop was negligible, so pressure applied at outlet did not influence on the velocity field. The temperature distribution showed that temperature variation along axial direction was small in the given average fluid velocity. Clearly, the heat conduction from the wall was not as fast as heat convection in axial direction. The catalyst-bed temperature was governed by the temperature at the inlet. The heat from the exothermic reaction was also minor. The CO concentration distribution showed slightly higher concentration towards the axis, due to high diffusion of mass and/or high reaction rate caused by heat from the wall. By comparing temperature and mass distributions, one can tell that diffusion to advection (mass) is relatively higher than conduction to convection (heat).

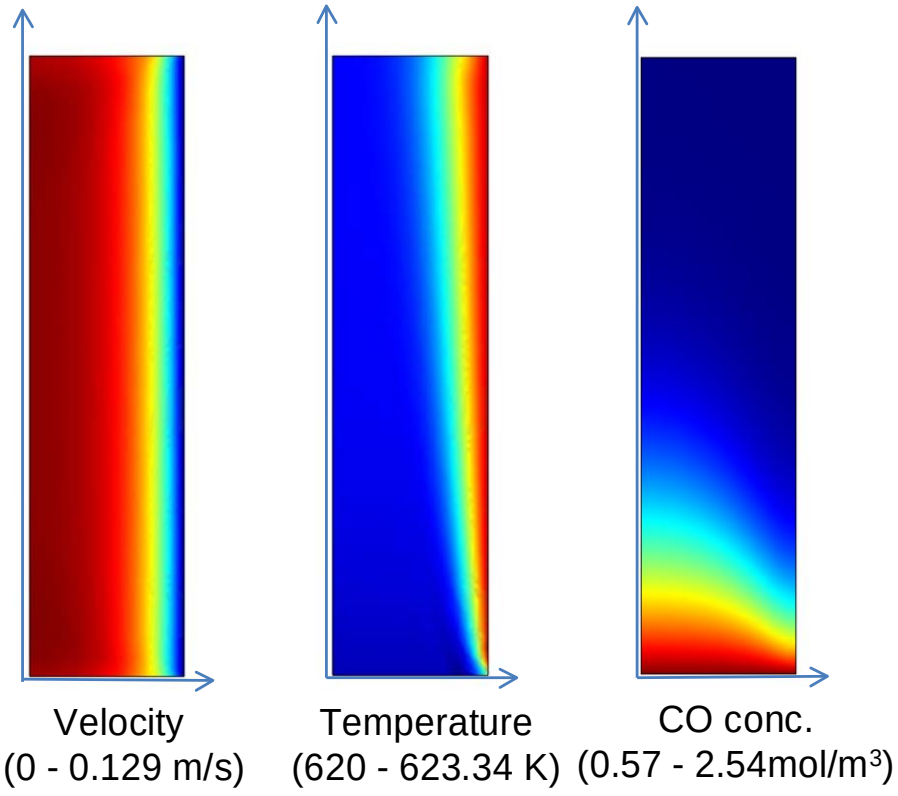

Figure 2 Distribution of velocity, temperature, mass in cross-section through the z-axis

5. Validation

Validity of the simulation was checked by simple calculations of pressure drop in the reactor. From Darcy's law, average flow rate is expressed as Equation 11, where κ is permeability, η is dynamic viscosity, and L is the length of the reactor. Since the average velocity at the inlet was set to 0.085 m/s, pressure gradient, $\triangle$p/ L was calculated to be 8.5 Pa/m. This pressure gradient is very small compared to the atmospheric pressure and consistent with the obtained pressure difference between the inlet and the outlet, 1.00001×10^5 Pa.

$$\langle v \rangle = -\left(\kappa / \eta \right) \left(\triangle p / L \right) \qquad \text{(Equation 11)}$$

Validity of the simulation was also checked by CO concentration at equilibrium. From Equation 7 and equilibrium constant of 21.34 for reaction temperature (623.15 K), CO concentration is calculated to be 0.566 mol/m^3, which is consistent with the simulated result.

The maximum Reynolds number (R_e) inside the reactor ranged from 0.2 to 2.7, which indicates the system is stable. Since characteristic mesh length L was around 2×10^{-4} m, estimated Re from Equation 12 is 0.4, which is within the range obtained from the simulation. Peclet number (P_e) for mass transfer ranged from 0.1 to 1.5, which is also low enough for the simulation to converge. The estimated P_e from Equation 13 is 0.3, which is also in good agreement with simulation.

$$R_e = \rho \, v_{avg} \, L / \eta \qquad \text{(Equation 12)}$$

$$P_e = v_{avg} \, L / D \qquad \text{(Equation 13)}$$

6. Parametric study

The effects of parameters, average flow rate (U_0), heat of reaction ($\triangle H$), permeability (κ), and porosity (ε), on fluid behavior were investigated.

6-1. Effect of average linear velocity

Figure 3 is velocity – radial distance plot at the middle of catalyst-bed length. As the average flow rate (U_0) increased, velocity became more dependent on radial distance. In laminar flow, the maximum velocity at z-axis is twice of U_0. With the porous media, the maximum velocity was always 1.5 times of U_0. Note that the flow was well developed at the middle of catalyst-bed length. The dependence of temperature and CO concentration on U_0 were also plotted in Figure 4. The inlet temperature was carried through the entire catalyst-bed when U_0 > 0.05 m/s while heat conduction became effective when U_0 < 0.01 m/s. Likewise, CO concentration stayed higher level when U_0 is high, it quickly decreased when U_0 is small. However, as pointed out in the section 4, temperature is more affected by convection than CO concentration.

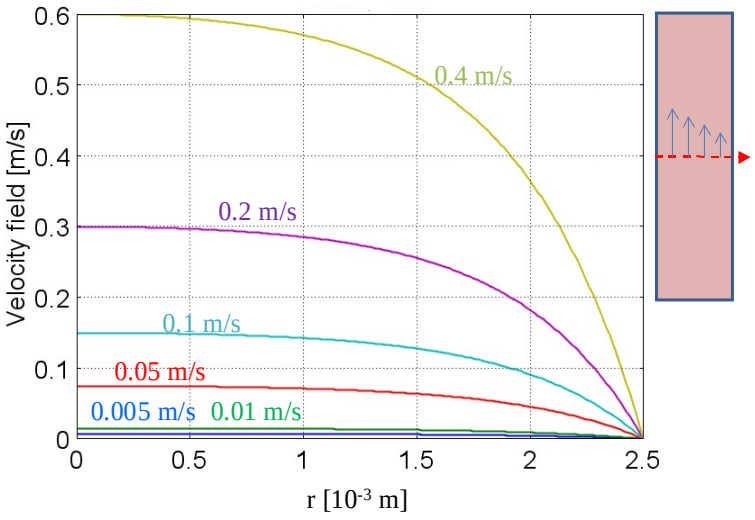

Figure 3 Effect of average flow rate on z-velocity

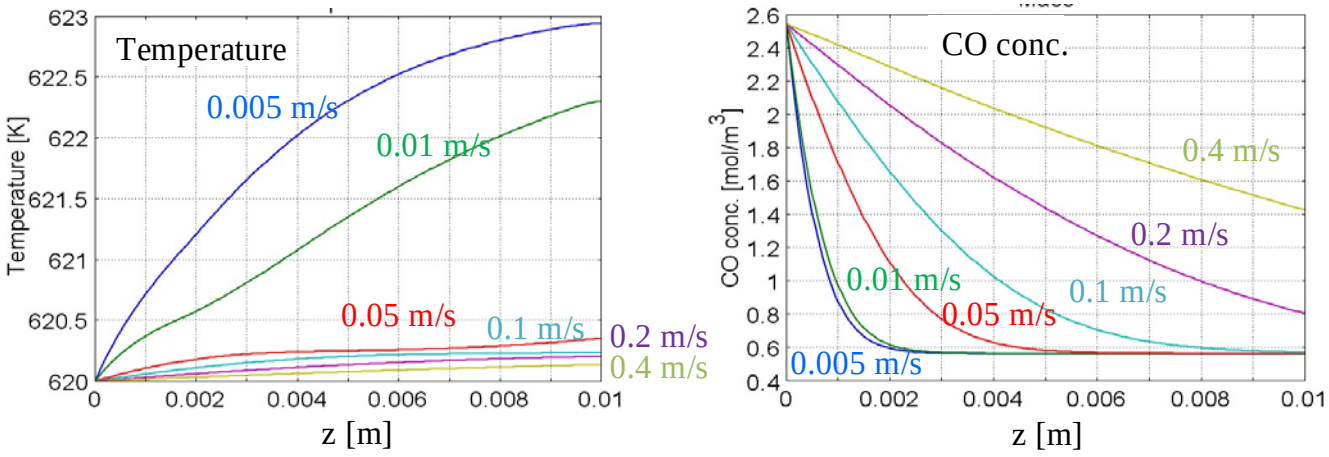

Figure 4 Effect of average flow rate on temperature and CO concentration

6-2. Effect of heat of reaction

Heat of reaction ($\triangle H$) was varied from slightly endothermic (+20kJ/mol) to highly exothermic (-400kJ/mol). Figure 5 shows that $\triangle H$ does not have much effect on temperature. Even the most exothermic reaction increased the bed temperature only by a few degrees. Accordingly, water gas shift reaction was not affected by $\triangle H$.

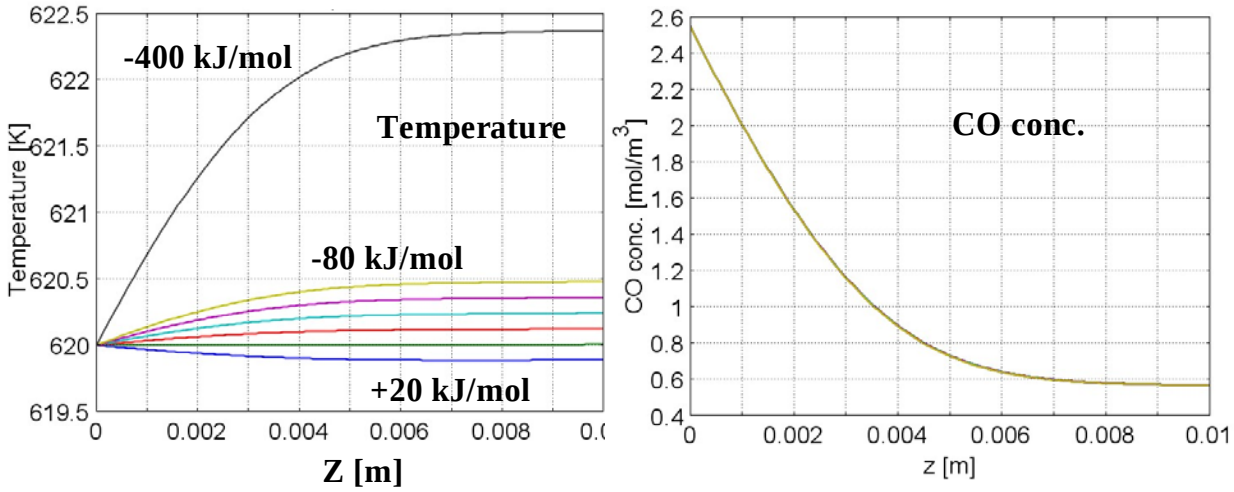

Figure 5 Effect of heat of reaction on temperature and CO concentration

6-3. Effect of properties of porous media (permeability and porosity)

The effect of permeability (κ) was tested and the result was plotted as radial profile at the middle of the bed length (Figure 6). When κ is 10^{-6} m^2, the velocity profile was close to laminar flow. As κ decreases, the velocity along radial direction becomes flat. Temperature did not change so much. This would be due to effect of convection is larger than heat conduction. The CO concentration was also flattened since advective term was suppressed.

The effect of porosity (ε) was also tested (Figure 6). Thermal conductivity, heat capacity, and diffusivity were changed according to Equation 8-10. The result showed the similar trend as porosity, i.e. velocity and CO concentration distribution were flattened while temperature distribution was not affected much, although its impact was smaller than that of permeability. Figure 7 is the plot of pressure drop through the bed length. This figure clearly shows the large impact of permeability.

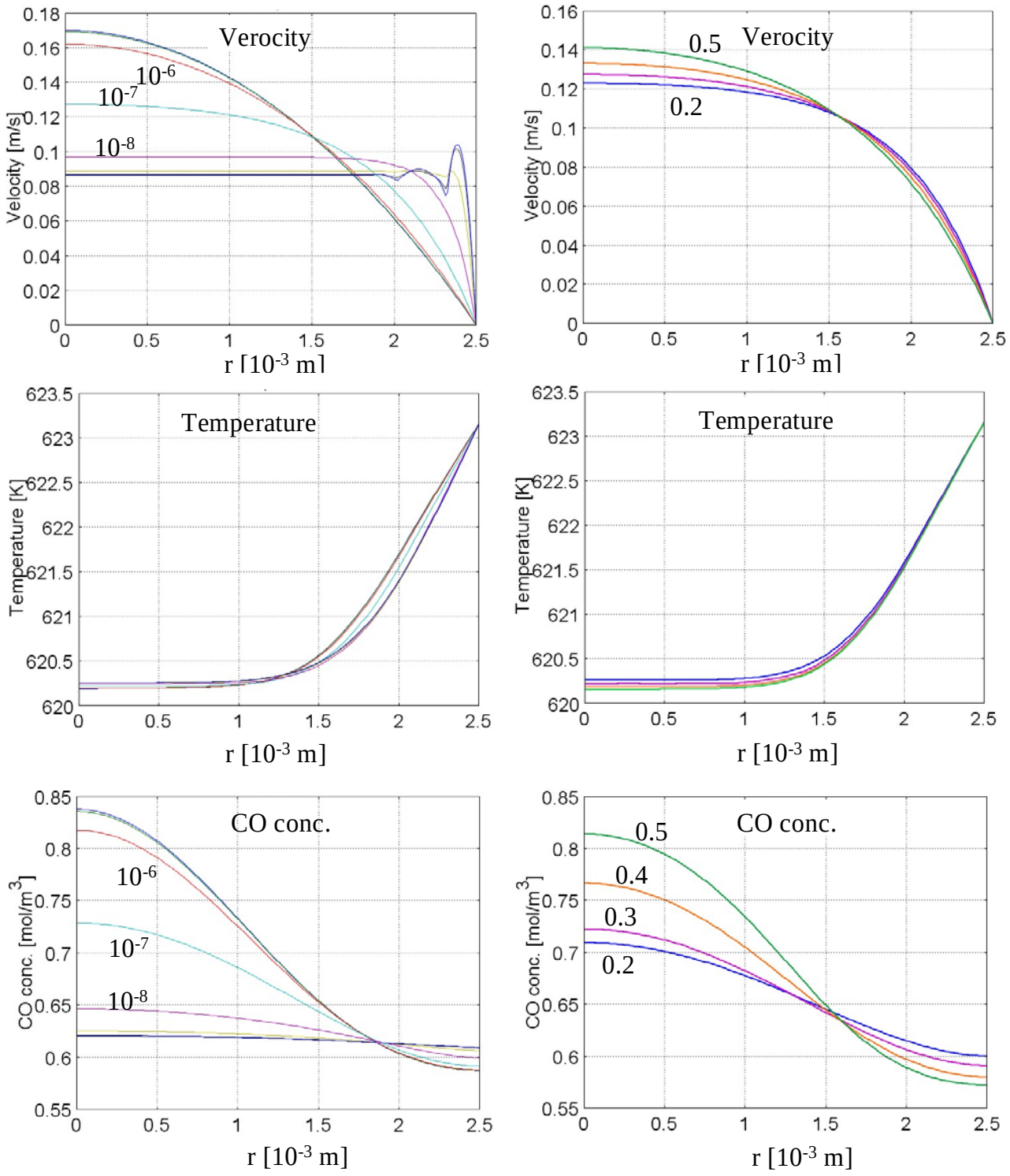

Figure 6 Effect of permeability (left) and porosity (right)

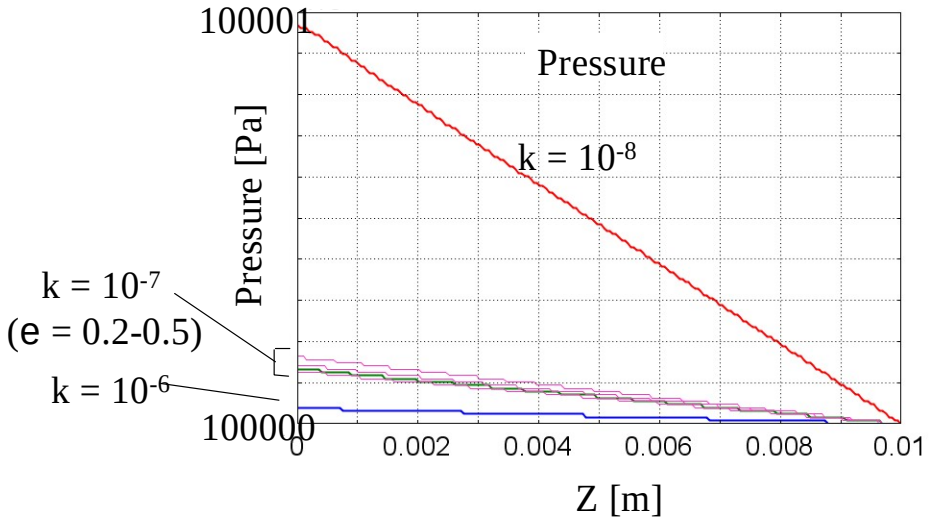

Figure 7 Effect of permeability and porosity on pressure

7. Detailed fluid behavior in particle scale

To demonstrate that the mass diffusion effectively homogenizes uneven velocity field of the fluid, simulation on particle model was also conducted. The model and the result were shown in Figure 8. Two-dimensional model was used and temperature was assumed constant (623.15 K). The particle diameter was set to 500 μ m. The different parameters were applied for gas and porous particle. Permeability was set to 10^{-11} m^2, ten thousand times lower than the plug flow model. Porosity was set to 0.2, which is the minimum of realistic condition. Mass diffusivity was changed to 0.5 x 10^{-5} m^2/s according to Table 1. The result indicated the variation of CO concentration along radial direction is effectively suppressed by diffusion. When combining heat balance calculation was also attempted, however, temperature showed unstable behavior at the edge of the particle. (When permeability was decreased to 10^{-14}, temperature behavior seemed reasonable.)

8. Conclusion

An actual water gas shift reactor was reproduced in simulation of momentum, heat, and mass transfer using COMSOL. The result was validated by pressure drop of the reactor and mass concentration at equilibrium. Convective term was dominant in heat transfer while both advective and diffusive terms are influential in mass transfer. The catalyst-bed temperature was almost same

as the inlet temperature throughout the reactor length in the given condition. Permeability had a large impact on homogeneity of fluid. Gas diffusion effectively flattened mass distribution from uneven fluid flow in the particle model.

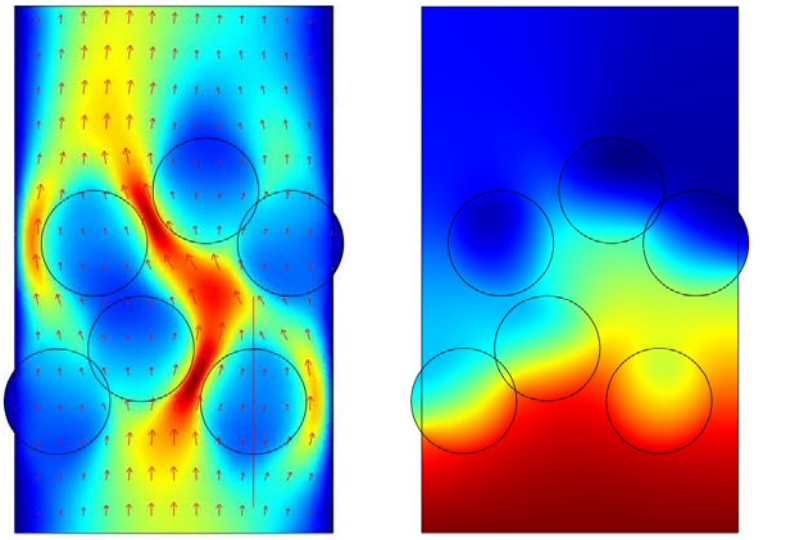

Velocity (0~0.22 m/s) CO conc. (2.54~1.67 mol/m^3)

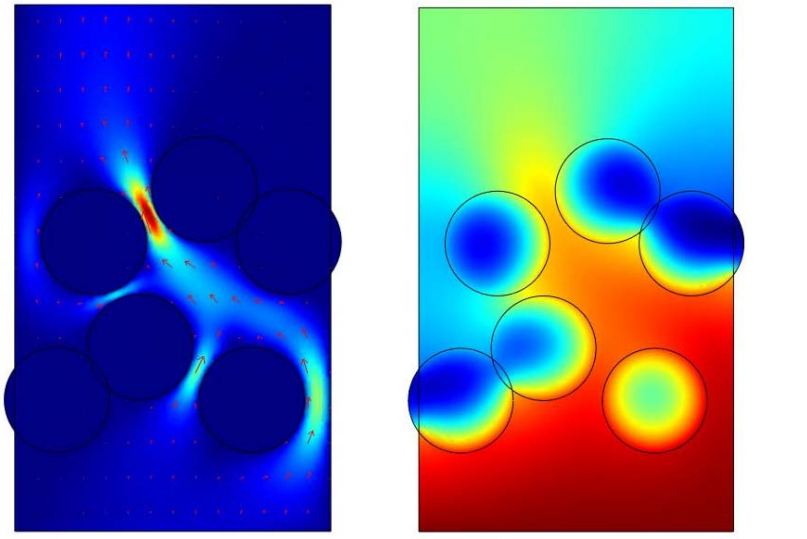

Velocity (0~1.66 m/s) CO conc. (2.54~1.14 mol/m^3)

Figure 8 Velocity and CO concentration map in 2D particle model
Upper: $\kappa = 10^{-9}$, $\varepsilon = 0.4$
Lower: $\kappa = 10^{-11}$, $\varepsilon = 0.2$

References

[1] M. Nijemeisland, A. G. Dixon, and E. H. Stitt, "Catalyst design by CFD for heat transfer and reaction in steam reforming," *Chem Eng Sci*, vol. 59, pp. 5185-5191, 2004.

[2] A. G. Dixon, M. E. Taskin, E. H. Stitt, and M. Nijemeisland, "3D CFD simulations of steam reforming with resolved intraparticle reaction and gradients," *Chem Eng Sci*, vol. 62, pp. 4963-4966, 2007.

[3] J. R. Rostrup-Nielsen, J. Sehested, and J. K. Norskov, "Hydrogen and synthesis gas by steam- and CO2 reforming," *Adv Catal*, vol. 47, pp. 65-139, 2002.

[4] A. G. Dixon and M. Nijemeisland, "CFD as a design tool for fixed-bed reactors," *Ind Eng Chem Res*, vol. 40, pp. 5246-5254, 2001.

[5] H. M. Kvamsdal, H. F. Svendsen, T. Hertzberg, and O. Olsvik, "Dynamic simulation and optimization of a catalytic steam reformer," *Chem Eng Sci*, vol. 54, pp. 2697-2706, 1999.

[6] A. G. Dixon and D. L. Cresswell, "Theoretical Prediction of Effective Heat-Transfer Parameters in Packed-Beds," *Aiche J*, vol. 25, pp. 663-676, 1979.

[7] D. G. Bunnell, H. B. Irvin, R. W. Olson, and J. M. Smith, "Effective Thermal Conductivities in Gas-Solid Systems," *Ind Eng Chem*, vol. 41, pp. 1977-1981, 1949.

[8] M. Nijemeisland and A. G. Dixon, "Comparison of CFD simulations to experiment for convective heat transfer in a gas-solid fixed bed," *Chem Eng J*, vol. 82, pp. 231-246, 2001.

[9] A. G. Dixon and D. L. Cresswell, "Estimation of Heat-Transfer Parameters in Packed-Beds from Radial Temperature Profiles - Comment," *Chem Eng J Bioch Eng*, vol. 17, pp. 247-248, 1979.

[10] L. F. Gladden, "Recent advances in MRI studies of chemical reactors: ultrafast imaging of multiphase flows," *Top Catal*, vol. 24, pp. 19-28, 2003.

[11] J. Park and S. J. Gibbs, "Mapping flow and dispersion in a packed column by MRI," *Aiche J*, vol. 45, pp. 655-660, 1999.

[12] E. H. L. Yuen, A. J. Sederman, F. Sani, P. Alexander, and L. F. Gladden, "Correlations between local conversion and hydrodynamics in a 3-D fixed-bed esterification process: An MRI and lattice-Boltzmann study," *Chem Eng Sci*, vol. 58, pp. 613-619, 2003.

[13] L. F. Gladden, M. D. Mantle, A. J. Sederman, and E. H. L. Yuen, "Magnetic resonance imaging of single- and two-phase flow in fixed-bed reactors," *Appl Magn Reson*, vol. 22, pp.

201-212, 2002.

[14] I. Ziolkowska and D. Ziolkowski, "Modelling of gas interstitial velocity radial distribution over cross-section of a tube packed with granular catalyst bed; effects of granule shape and of lateral gas mixing," *Chem Eng Sci*, vol. 62, pp. 2491-2502, 2007.

[15] H. P. A. Calis, J. Nijenhuis, B. C. Paikert, F. M. Dautzenberg, and C. M. van den Bleek, "CFD modelling and experimental validation of pressure drop and flow profile in a novel structured catalytic reactor packing," *Chem Eng Sci*, vol. 56, pp. 1713-1720, 2001.

[16] M. Nijemeisland and A. G. Dixon, "CFD study of fluid flow and wall heat transfer in a fixed bed of spheres," *Aiche J*, vol. 50, pp. 906-921, 2004.

[17] S. A. Logtenberg and A. G. Dixon, "Computational fluid dynamics studies of fixed bed heat transfer," *Chem Eng Process*, vol. 37, pp. 7-21, 1998.

[18] A. G. Dixon, M. Nijemeisland, and E. H. Stitt, "CFD study of heat transfer near and at the wall of a fixed bed reactor tube: Effect of wall conduction," *Ind Eng Chem Res*, vol. 44, pp. 6342-6353, 2005.

[19] M. E. Taskin, A. G. Dixon, and E. H. Stitt, "CFD study of fluid flow and heat transfer in a fixed bed of cylinders," *Numer Heat Tra-Appl*, vol. 52, pp. 203-218, 2007.

[20] T. Zeiser, M. Steven, H. Freund, P. Lammers, G. Brenner, F. Durst, and J. Bernsdorf, "Analysis of the flow field and pressure drop in fixed-bed reactors with the help of lattice Boltzmann simulations," *Philos T Roy Soc A*, vol. 360, pp. 507-520, 2002.

[21] Delhaye, J. M. and Achard, J. L. (Eds.: Banerjee, S. and Weaver, K. R.) *Transient two-phase flow* Vol. 1 (1976) pp.5–84 AECL, Canada.